

## Geotropic tracers in turbulent flows: a proxy for fluid acceleration

F. De Lillo<sup>a\*</sup>, M. Cencini<sup>b</sup>, G. Boffetta<sup>a</sup> and F. Santamaria<sup>a</sup>

<sup>a</sup>*Dip. di Fisica and INFN, Università di Torino, via P.Giuria 1, 10125 Torino, Italy;* <sup>b</sup>*Istituto dei Sistemi Complessi, CNR, via dei Taurini 19, 00185 Rome, Italy*

(Received 21 December 2012; accepted 19 July 2013)

We investigate the statistics of orientation of small, neutrally buoyant, spherical tracers whose centre of mass is displaced from the geometrical centre. If appropriate-sized particles are considered, a linear relation can be derived between the horizontal components of the orientation vector and the same components of acceleration. Direct numerical simulations are carried out, showing that such relation can be used to reconstruct the statistics of acceleration fluctuations up to the order of the gravitational acceleration. Based on such results, we suggest a novel method for the local experimental measurement of accelerations in turbulent flows.

**Keywords:** isotropic turbulence; homogeneous turbulence; direct numerical simulation; experimental techniques

### 1. Introduction

The Lagrangian investigation of turbulence has dramatically improved in the last few years in experimental techniques, theoretical models and numerical simulations [1]. These progresses benefited from the increased range of Reynolds numbers accessible for investigation (in particular, for simulations) and the improved accuracy of measurement techniques. On the theoretical side, we have now phenomenological models able to quantitatively explain the Lagrangian properties of turbulence such as the statistics of velocity increments [2] and accelerations [3]. Grounded on the successes of Lagrangian investigations, recent experimental and numerical studies started to investigate the motion of complex objects in turbulent flows [4–9]. The motivations are both fundamental and applicative. In this short note, we suggest a possible technique to measure turbulent accelerations without the need of particle tracking, by means of the local measurement of the orientation of finite-size particles. The idea relies on spherical particles whose average density is that of the carrier fluid (so that they are neutrally buoyant), but whose centre of mass is displaced with respect to the geometrical centre (implying that the orientation is determined by the gravitational torque and that due to the fluid). By means of direct numerical simulations (DNS), we show that information on particle orientation can be used to estimate fluid accelerations up to the order of gravitational acceleration.

The paper is organised as follows. In Section 2, we discuss the theoretical basis of the technique in its simplest implementation. Section 3 presents some preliminary validation of the method based on numerical simulations. Finally, Section 4 is devoted to conclusions and perspectives.

---

\*Corresponding author. Email: [delillo@to.infn.it](mailto:delillo@to.infn.it)

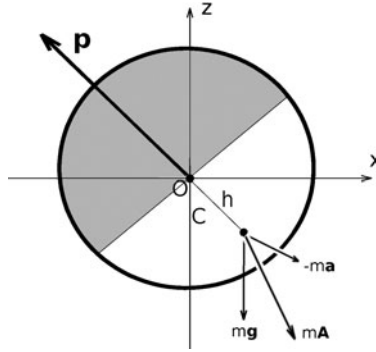


Figure 1. An example of geotropic particle with black and white pattern. Forces are represented as measured in the reference frame of the particle's centre. Acceleration of the particle by the fluid (which is due to surface forces acting on the geometrical centre of the body) produces in this non-inertial frame an apparent force added to gravity and acting on the centre of mass.

## 2. The motion of geotropic tracers

We consider the trajectory,  $\mathbf{x}(t)$ , of a neutrally buoyant sphere small enough such that its dynamics can be approximated by that of a passive tracer,

$$\frac{d\mathbf{x}}{dt} = \mathbf{u}(\mathbf{x}, t), \quad (1)$$

transported by a flow  $\mathbf{u}(\mathbf{x}, t)$ . As sketched in Figure 1, we assume that the particle centre of mass  $C$  is displaced by a distance  $h$  with respect to the geometrical centre  $O$  (which is the centre of buoyancy). The displacement determines the particle orientation, defined by the unit vector  $\mathbf{p}$  directed opposite to the centre of mass. The direction  $\mathbf{p}$  is determined by the balance between the different torques acting on the particle. Because of particle asymmetry, an external force  $\mathbf{f}$  acting on the centre of mass such as gravity  $m\mathbf{g}$ , results in a torque  $\mathbf{T}_f = -h\mathbf{p} \times \mathbf{f}$ . In addition, the particle immersed in a fluid experiences a viscous torque  $\mathbf{T}_v = 8\pi\nu\rho r^3(\boldsymbol{\omega}/2 - \boldsymbol{\Omega})$ , where  $\boldsymbol{\omega} = \nabla \times \mathbf{u}$  is the fluid vorticity,  $\nu$  and  $\rho$  are the fluid kinematic viscosity and density, respectively, and  $\boldsymbol{\Omega}$  is the angular velocity of the sphere. If the particle Reynolds number is very small, we can assume creeping flow conditions around the sphere, which impose equilibrium between the external forces and the viscous ones, in this particular case zero total torque  $\mathbf{T}_f + \mathbf{T}_v = 0$ . From the solid body rotation formula  $\dot{\mathbf{p}} = \mathbf{p} \times \boldsymbol{\Omega}$  and  $\mathbf{p} \times (\mathbf{T}_f + \mathbf{T}_v) = 0$ , we end with the following equation for the orientation [10]:

$$\frac{d\mathbf{p}}{dt} = -\frac{1}{2v_0} [\mathbf{A} - (\mathbf{A} \cdot \mathbf{p})\mathbf{p}] + \frac{1}{2}\boldsymbol{\omega} \times \mathbf{p}, \quad (2)$$

where  $\mathbf{A}$  has the dimension of an acceleration and denotes the sum of gravity and inertial forces per unit mass, as measured in the reference frame of the sphere. The constant  $v_0 = 3\nu/h$ , having the dimension of a velocity, weighs the contribution of external forces to particle orientation. We remark that in the case of axisymmetric non-spherical particles an additional term is present in (2) [8–10].

Equations (1) and (2) are valid in the limit of small, neutrally buoyant particles. If inertia is taken into account, particle motion is described by integro-differential equations

containing added mass and history effects (see Ref. [11]). No such effects will be considered here, consistently with our approximations. In a fluid at rest, fluid acceleration and vorticity vanish and the only external force entering Equation (2) is gravity, so that  $\mathbf{A} = \mathbf{g} = (0, 0, -g)$ . Consequently, Equation (2) predicts that particles orient upwards with a relaxation time  $\mathcal{O}(v_0/g)$ . Such phenomenon is well known in bio-fluid-dynamics and is at the basis of the ability of some bottom-heavy phytoplankters to swim towards the sea surface (a phenomenon dubbed *negative gravitaxis* [10]), maximising the exposition to light and thus the photosynthetic activity.

In a turbulent flow, advected particles are subject to intense accelerations, so that, locally, gravity must be corrected due to inertial forces. The total acceleration  $\mathbf{A}$  acting on the particle is thus given by  $\mathbf{A} = \mathbf{g} - \mathbf{a}$ , where  $\mathbf{a} = d\mathbf{u}/dt$  is the fluid acceleration at the particle position. Again, the assumption that the acceleration of the particle is equal to that of the fluid implies particles smaller than few  $\eta$ . Numerical [12,13] and experimental [14,15] investigations showed that particles larger than  $\eta$  sense accelerations smaller than tracers. If one restricts to diameters up to  $4\eta$  the error on the rms value should be less than 20%. There is indication that such larger particles can accurately be described by including Faxen's corrections in the equation of motion [12,13].

In the following, for the sake of simplicity, we assume that fluid acceleration is smaller than gravity, i.e.  $g \gg a_{\text{rms}}$ . This is true for flows at moderate Reynolds numbers only [16], but this assumption greatly simplifies the analysis of (2). Formally, we can write  $\mathbf{A} = \mathbf{g} - \epsilon \mathbf{a}$  in Equation (2), with  $\epsilon$  a small nondimensional number. Further we consider the limit of fast reorientation, which amounts to requiring that the reorientation time  $v_0/g$  is smaller than the Kolmogorov time  $\tau_\eta$ . If one estimates  $a_{\text{rms}} \sim \epsilon^{3/4}/\nu^{1/4}$  and assumes  $h \sim \eta$  in the definition of  $v_0$ , fast orientation consistently implies  $g \gg a_{\text{rms}}$ .

When the vortical term  $\boldsymbol{\omega} \times \mathbf{p}$  is small, i.e. when  $v_0\omega_{\text{rms}} \ll a_{\text{rms}}$ , Equation (2) reduces to  $\mathbf{A} = (\mathbf{A} \cdot \mathbf{p})\mathbf{p}$ , which explicitly reads

$$\begin{aligned}\epsilon a_x &= (\epsilon \mathbf{a} \cdot \mathbf{p} + g p_z) p_x, \\ \epsilon a_y &= (\epsilon \mathbf{a} \cdot \mathbf{p} + g p_z) p_y, \\ \epsilon a_z + g &= (\epsilon \mathbf{a} \cdot \mathbf{p} + g p_z) p_z.\end{aligned}\tag{3}$$

From (3) one can see that the orientation vector must have the form  $\mathbf{p} = (\epsilon q_x, \epsilon q_y, 1)$ , indeed as  $p^2 = 1$  the correction to  $p_z$  will be  $\mathcal{O}(\epsilon^2)$  so that we can neglect it at this level. Plugging the expression for  $\mathbf{p}$  in Equation (3), at  $\mathcal{O}(\epsilon)$  we obtain  $\mathbf{q} = (a_x/g, a_y/g, 0)$ . In conclusion, from the orientation of the particle with respect to the vertical we can measure two components of the fluid acceleration

$$\mathbf{p} = \left( \frac{a_x}{g}, \frac{a_y}{g}, 1 \right).\tag{4}$$

This result is valid under the assumption that  $a_{\text{rms}} \ll g$  and, therefore, in general for not too high Re. This condition together with the smallness of the vorticity term implies fast orientation ( $v_0/g \ll \tau_\eta$ ). As a consequence, if  $v_0$  is too large, the first effect we expect is that vorticity becomes relevant, with an increase of the tilting angle, so that using (4) could lead to an over-estimate of accelerations. In more general conditions, it is in principle still possible to use (2) to gather information on the acceleration statistics but this requires less direct procedures, which we will not consider in this preliminary study.

Table 1. Parameters of the simulations made dimensional on the basis of laboratory experiments at similar Reynolds numbers [7,14].

$Re_\lambda$	$\eta$ (m)	$\tau_\eta$ (s)	$u_{\text{rms}}$ ( $\text{ms}^{-1}$ )	$\epsilon$ ( $\text{m}^2\text{s}^{-3}$ )	$L$ (m)	$a_{\text{rms}}$ ( $\text{ms}^{-2}$ )	$T$ (s)
200	$191 \times 10^{-6}$	$37 \times 10^{-3}$	0.037	$7.1 \times 10^{-4}$	0.07	0.24	8.22
400	$98 \times 10^{-6}$	$9.5 \times 10^{-3}$	0.097	$9.1 \times 10^{-3}$	0.10	1.5	2.58

Notes:  $\eta = (\nu^3/\epsilon)^{1/4}$  is the Kolmogorov scale,  $\tau_\eta = (\nu/\epsilon)^{1/2}$  is the Kolmogorov time,  $u_{\text{rms}}$  is the root mean square of the velocity,  $\epsilon$  is the energy dissipation per unit mass,  $L = u_{\text{rms}}^3/\epsilon$  is the integral length scale,  $a_{\text{rms}}$  is the root mean square acceleration.  $T$  is the integration time. For both simulations  $g = 9.8 \text{ ms}^{-2}$ .

### 3. Numerical simulations of geotropic tracers in turbulence

In this section, we illustrate the behaviour of geotropic particles in realistic turbulent flows and explore the range of validity of the result (4) by means of DNS of the dynamics of geotropic tracers together with the Navier–Stokes equations for an incompressible flow. Trajectories (up to  $2 \times 10^5$ ) are stored together with  $\mathbf{a}$  and  $\boldsymbol{\omega}$  in statistically stationary conditions. Equation (2) is then integrated starting from random orientations and for different values of  $v_0$ . After an initial transient of the order of  $v_0/g$ , during which particles forget their initial orientation, we can compare the acceleration  $\mathbf{a}$  with the prediction of Equation (4).

We have performed simulations of homogeneous-isotropic turbulence by means of a parallel pseudo-spectral code in a cubic box with periodic boundary conditions at  $Re_\lambda \simeq 200$  with resolution  $512^3$ . Statistical stationarity was maintained via a Gaussian, delta-correlated in time, random forcing at small wave-numbers. Equation (1) is integrated evaluating the velocity at particle position by means of trilinear interpolation. Moreover, we have also exploited a database [17] of previously simulated Lagrangian trajectories at resolution  $2048^3$  and  $Re_\lambda \simeq 400$ , for which acceleration and vorticity were available. Equation (2) was integrated using a second-order Adams–Bashforth scheme. In order to get physical relevance from the DNS, we rescale space and time with dimensional values. This is easily done by matching the Kolmogorov scale and time with experimental values at similar  $Re_\lambda$ , as shown in Table 1. We remark that this rescaling is not unique as  $Re_\lambda$  fixes a ratio of scales (and times) and not an absolute scale. This point is crucial as the parameter  $v_0$  is limited by the size of the particle and  $g$  is obviously fixed. In the following, we use laboratory experiments with an integral scale of the order of few cm for rescaling our simulations to physical values [7,14].

Figure 2 shows an example of time series of the two components of the acceleration  $a_x$  and  $a_y$  obtained following a Lagrangian tracer in the flow at  $Re_\lambda = 200$ . The initial condition of the orientation is along the  $z$ -axis,  $\mathbf{p}(0) = (0, 0, 1)$ . The dashed red line represents the acceleration obtained according to (4) from the  $x$ -component of the orientation vector,  $a_x = gp_x$  of a particle with  $v_0 \simeq 0.006 \text{ ms}^{-1}$ . The corresponding relaxation time under gravity is  $\tau = v_0/g \simeq 6 \times 10^{-4} \text{ s}$ . In this case  $a_{\text{rms}} \ll g$  and, therefore, the estimation (4) is fully justified and indeed the acceleration is reproduced quite accurately.

In Figure 3, we show an example for a trajectory in a turbulent flow at  $Re_\lambda = 400$ . Although the rms of acceleration  $a_{\text{rms}} \simeq \epsilon^{3/4} \nu^{-1/4}$  is smaller than  $g$ , particles experience fluctuations comparable to, or even larger than  $g$ , where the assumptions leading to (4) are not applicable. These large fluctuations of Lagrangian acceleration are typical in turbulence and physically correspond to event of trapping of tracers in small scale vortices [3,16,18].

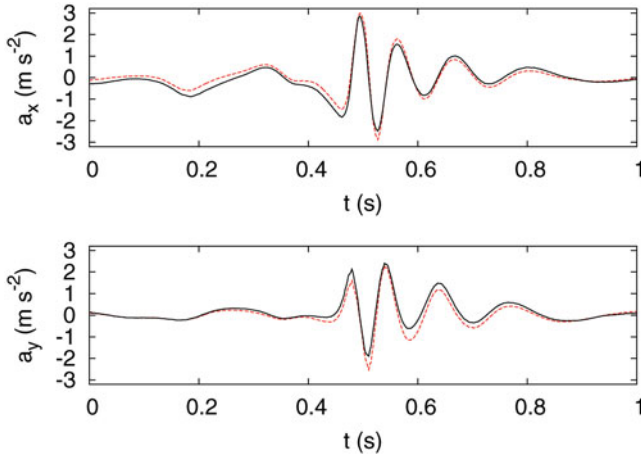


Figure 2.  $x$ -component (top) and  $y$ -component (bottom) of the acceleration of one particle computed from numerical simulations at  $Re_\lambda = 200$  (black line) together with the acceleration estimated from the  $x$ - and  $y$ -component of the orientation vector, i.e.  $a_x = gp_x$ ,  $a_y = gp_y$  see (4), of a geotropic particle with  $v_0 = 6 \text{ mm s}^{-1}$  corresponding to a displacement  $h = 0.5 \text{ mm}$ .

As shown in Figure 3, during these events the orientation vector  $\mathbf{p}$  is unable to accurately follow the acceleration fluctuation, which results to be slightly underestimated.

On a more quantitative level, Figure 4 shows the probability density function (PDF) of acceleration compared with the estimation obtained via (4). For each value of  $Re_\lambda$  considered, we simulate the results of three hypothetical experiments, with particles of different sizes. As discussed above, geotropic orientation is expected to be a good proxy for acceleration only in the limit of small  $v_0$ , i.e. for fast orientation. As apparent from both panels in Figure 4, when a large enough displacement  $h$  is considered, the statistics of acceleration is reproduced remarkably well by particle orientation. However, this is not the

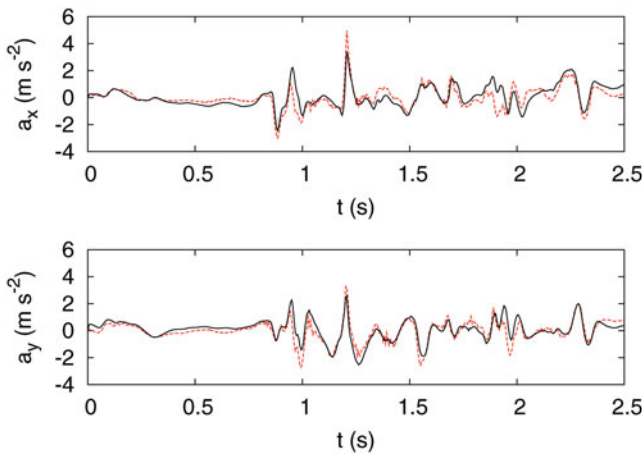


Figure 3. The same of Figure 2 for a geotropic trajectory with  $h = 0.2 \text{ mm}$  and  $v_0 = 15 \text{ mm s}^{-1}$  in a turbulent flow at  $Re_\lambda = 400$ .

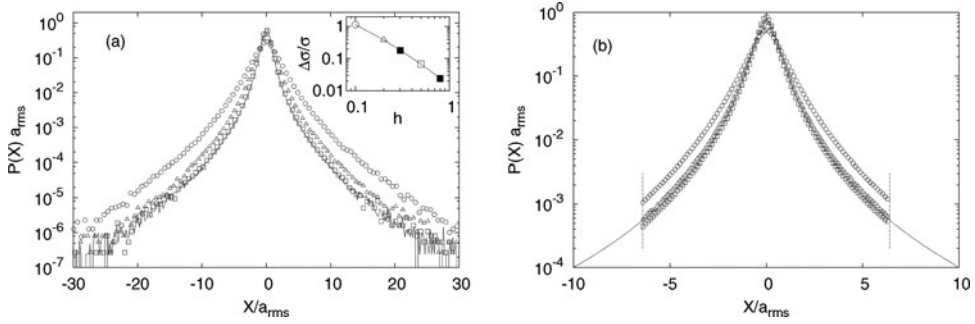


Figure 4. PDFs of acceleration in one horizontal direction for  $Re_\lambda = 200$  (a) and  $Re_\lambda = 400$  (b). Estimates obtained according to (2) ( $X = gp_x$ , symbols) are compared with fluid acceleration ( $X = a_x$ , line). Three values of particle bias were used, which rescaled on experimental values correspond to  $h = 0.1$  mm (circles), 0.2 mm (triangles) and 0.5 mm (squares). By comparison, it is evident that the intermediate value gives a good estimate at higher  $Re_\lambda$  but is not satisfying at the lower one (see the text). In (b) the value of  $g$  (vertical lines) marks the upper cut-off for measurable accelerations. In the inset of (a): relative error on the estimate of  $\sigma = \sqrt{\langle a_x^2 \rangle}$  as a function of  $h$ , for  $Re_\lambda = 200$ ,  $\Delta\sigma = g\sqrt{\langle p_x^2 \rangle} - \sigma$ .

case if less biased particles are considered. This clearly implies a *lower* limit in the size of particles used, a factor that must be taken into account in the design of possible experiments. As mentioned above, vorticity can be neglected only if  $v_0\omega_{rms}/a_{rms} \sim v_0/\delta u_\eta < 1$ . By applying the definition of the Kolmogorov scale  $\delta u_\eta\eta/\nu = 1$  and that of  $v_0$ , the constraint reduces (a part from order-one coefficients) to  $\eta \lesssim h$ . This inequality can pose a problem both for the validity of (1) and the actual statistics seen by the particle. Both points will be discussed in the final section. As for now we will just consider this condition in the framework of our model, assuming that the corrections are small as long as the particle size is of the same order as  $\eta$ .

If (as in our case) one considers a set of experiments all using water and with comparable integral scales, an increase in  $Re$  corresponds to a smaller viscous scale, thus decreasing the minimum particle size required to reconstruct acceleration. As an example of this, we considered the case of particles with  $h = 0.2$  mm. As evident from Figure 4 using Equation (4) on statistics obtained with such particles would lead to an overestimate of larger accelerations at  $Re_\lambda = 200$  (triangles in Figure 4a) while they would be acceptable candidates at  $Re_\lambda = 400$  (triangles in Figure 4(b)). However, the largest acceleration that can be measured by means of (2) is  $g$ . For experiments at higher  $Re$  where very large accelerations are present, this introduces a cut-off in the estimated accelerations. As evident from the results at  $Re_\lambda = 400$ , the core of the PDF is approximately correct, even if values above  $0.5 \div 0.7g$  are under-represented. We stress that the simulations exhibited accelerations up to  $80a_{rms}$  (not shown for graphical reasons), while  $g \approx 6.3a_{rms}$  if rescaled over the experimental parameters. Analysis of the variance of acceleration performed for  $Re_\lambda = 200$  (inset of Figure 4(a)) reveals that the second moment of the distribution is correctly recovered asymptotically in  $h/\eta$ . The same cannot be verified at  $Re_\lambda = 400$ , since the cut-off at  $g$  prevents convergence of the second moment of estimated accelerations.

In order to further investigate the errors on the estimate of the acceleration, we consider the joint distribution  $P(a_i, gp_i)$  (with  $i = x, y$ ) of each acceleration component and its estimate. As shown in Figure 5 such distributions confirm a tendency of smaller particles to

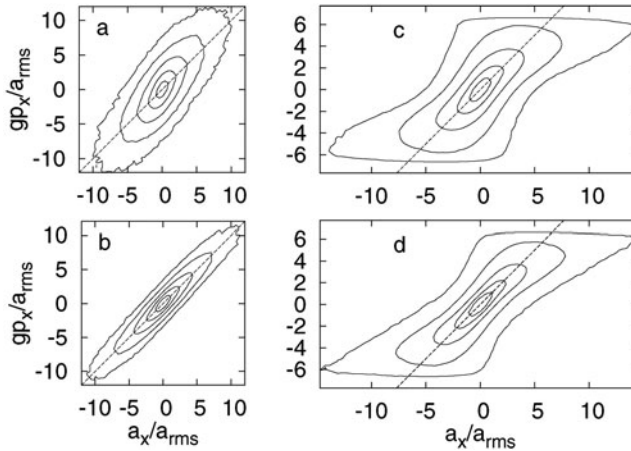


Figure 5. Joint PDF of acceleration and estimated acceleration for  $Re_\lambda = 200$  (a,b) and  $Re_\lambda = 400$  (c,d). Each panel refers to a different value of the displacement, 0.2 mm (a,c) and 0.5 mm (b,d). Contour levels are set a factor 10 apart starting from  $10^{-1}$  (at the centre) down. The straight line marks  $gp_x = a_x$  for reference. While the tendency is generally that of overestimating large accelerations (appearing as a clockwise tilt of the level sets), stronger ‘clockwise’ lobes appears for the larger displacement at  $Re_\lambda$  (d), compatible with the lower tails in the corresponding PDF of Figure 4. Note that the strong deformation of the PDF in (c) and (d) is due to the cut-off  $gp_x$ .

overestimate accelerations. Only for  $Re_\lambda = 400$  the largest particles underestimate accelerations, as can be seen by the low tails of the corresponding PDF in Figure 4 and by a slight asymmetry of  $P(a_x, gp_x)$  towards quadrants in which  $|gp_x| < |a_x|$ . The strongly intermittent nature of both acceleration and vorticity suggests to investigate in more detail how accurately accelerations of different magnitude can be estimated via (4). The conditional average  $\langle |1 - gp_x/a_x|; a_x \rangle$  is shown in Figure 6 for both values of  $Re_\lambda$ . Let us first consider the curves at  $Re_\lambda = 200$ . It is evident that larger particles (i.e. with faster reorientation time) provide better estimates: the largest particles, with  $h = 0.5$  mm give a minimum relative error of around 0.2. Through most of the observed range, the relative error is smaller for larger accelerations, because the effect of vorticity decreases accordingly. Indeed, the same figure also compares the relative error with  $v_0(\omega \times p)$ , showing that, for all but the largest accelerations, the error in the estimate comes from the vorticity term in (2), consistently with the assumption of fast orientation. For accelerations larger than  $\sim 0.1g$ , the effect of finite gravity causes deviations from this behaviour and eventually an increase of the relative error, as expected. This effect is less evident for smaller particles, most likely because they tend to overestimate the acceleration while the finite gravity effect leads to an underestimate so that there is a compensation between the two opposite effects. The right panel shows that the effect of finite gravity is much larger for  $Re_\lambda = 400$ , as expected. However, one should note that the vorticity term would give with the same particles a smaller error in this second case than for  $Re_\lambda = 200$ . Indeed, by estimating the error due to vorticity as  $v_0/u_\eta$  one would get a value about 1.9 smaller for the higher  $Re_\lambda$ , compatible within 10% with the numerical results around  $a \sim a_{rms}$ . We stress that this observation is not valid in general: it is a consequence of the fact that, in our case, the flow at higher Re has a larger effective integral scale and a larger  $u_\eta$ .

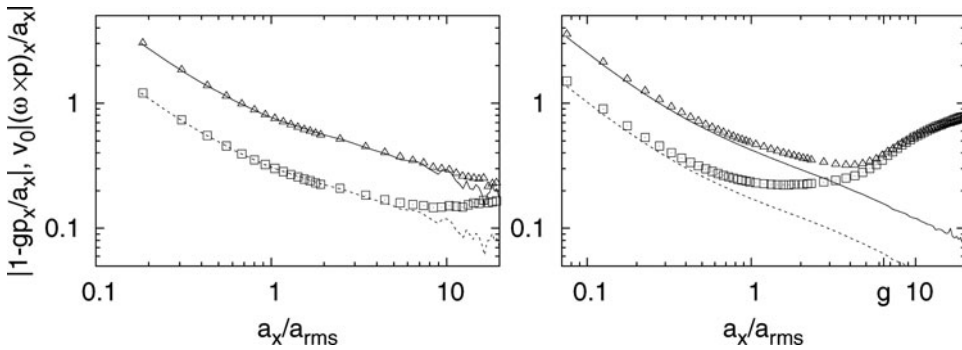


Figure 6. Relative error on the estimate of one component of acceleration by (4). The average  $\langle |1 - gp_x/a_x|; a_x \rangle$  conditioned on the local value of  $a_x$  (symbols) is compared with the contribution due to the vorticity term in (2)  $\langle v_0|\omega_y p_z - \omega_z p_y|; a_x \rangle$  (lines). For  $Re_\lambda = 200$  (left), the latter clearly constitutes the main contribution to the error. At  $Re_\lambda = 400$  (right), the estimate of larger accelerations is clearly affected by the finite value of  $g$ . Data refer to  $h = 0.2$  mm (triangles, solid line) and  $h = 0.5$  mm (squares, dotted line).

#### 4. Conclusion and discussion

Summarising our numerical results, it appears that the orientation of biased particles could be a viable proxy for fluid acceleration, at least at moderate  $Re$ . It is clearly important to establish a way to estimate the proper particle size based on the parameters of the turbulent flow to be examined.

Although particle size does not directly enter the model equations, the offset  $h$  clearly sets a lower bound on particle radius. This point must be carefully considered. Particles should be sufficiently biased to ensure dominance of acceleration leading over rotation due to vorticity, but too large particles would not obey the assumptions leading to (1) and (2).

On the other hand, experimental limitations should be considered. In order to use (4) to directly measure fluid acceleration one has to measure the tilt angle of a geotropic particle transported by the flow. One possibility is to use small spherical particles with the upper and lower hemisphere of different colors as in the example of Figure 1, a simpler version of the technique used in [4]. By measuring the angle  $\theta$  of the particle ‘equator’ with respect to the horizontal plane one has  $p_x = \sin \theta$ .

A precise determination of  $\theta$  requires sufficient resolution of the particle pattern and therefore not too small particles. On the other hand, because the measure is instantaneous, there is no need to follow the particles. Therefore, the camera could be placed to zoom a small region of the fluid only, and to acquire data when a particle comes in that region.

Let us finally comment about possible corrections to the described behaviour, for the two cases of particles too small or too large. If the offset  $h$  is too small, the vorticity term in (2) is no longer negligible. As a consequence, reconstruction of acceleration would require independent information on vorticity, so that a more complex method would be required. Furthermore, fast orientation is at the basis of (4) which allows one to avoid particle tracking, and would be important to follow high frequency fluctuations accurately. In the case of too large particles, the creeping flow assumption would be inaccurate. Nonetheless, the tilting angle would still provide information on the fluid acceleration but Equation (2) has to be modified to take inertial terms into account.

A further aspect that should be taken into account is finite size effects on particle trajectory. In general, one expects that particles larger than the Kolmogorov scale deviate

from fluid trajectories. However, there is evidence that acceleration statistics are not strongly influenced by particle size [12,13,15]. Numerical and experimental results suggest that addition of the so-called Faxen terms in the equation for particle trajectory can account for the main deviations, providing a method to estimate the related errors [12,13]. Such corrections should become relevant when the radius of the particle is larger than  $\eta\sqrt{\text{Re}_\lambda}$ , which for experiments comparable to the ones we considered would give  $O(10)\eta$  [12], thus allowing for some range of sizes to explore.

Given the above constraints, we can conclude that the proposed method would be reasonably accurate for typical experimental settings at moderate Reynolds numbers or when large Reynolds number are achieved thanks to a large integral scale. In spite of the above discussed limitations, we think that the idea of exploiting biased particles to measure acceleration without tracking may be interesting especially if technology can be pushed to the possibility to measure the tilting angle of many particles at the same time, allowing for the reconstruction of the spatial field of accelerations.

### Acknowledgement

The authors acknowledge support by the COST Action MP0806 and MIUR PRIN-2009PYYZM5

### References

- [1] F. Toschi and E. Bodenschatz, *Lagrangian properties of particles in turbulence*, Annu. Rev. Fluid Mech. 41 (2009), pp. 375–404.
- [2] A. Arneodo, R. Benzi, J. Berg, L. Biferale, E. Bodenschatz, A. Busse, E. Calzavarini, B. Castaing, M. Cencini, L. Chevillard, R.T. Fisher, R. Grauer, H. Homann, D. Lamb, A.S. Lanotte, E. Leveque, B. Luthi, J. Mann, N. Mordant, W.C. Muller, S. Ott, N.T. Ouellette, J-F. Pinton, S.B. Pope, S.G. Roux, F. Toschi, H. Xu, and P.K. Yeung, *Universal intermittent properties of particle trajectories in highly turbulent flows*, Phys. Rev. Lett. 100 (2008), p. 254504.
- [3] L. Biferale, G. Boffetta, A. Celani, B. Devenish, A. Lanotte, and F. Toschi, *Multifractal statistics of Lagrangian velocity and acceleration in turbulence*, Phys. Rev. Lett. 93 (2004), 64502.
- [4] R. Zimmermann, Y. Gasteuil, M. Bourgoïn, R. Volk, A. Pumir, and J.F. Pinton, *Rotational intermittency and turbulence induced lift experienced by large particles in a turbulent flow*, Phys. Rev. Lett. 106 (2011), p. 154501.
- [5] R. Zimmermann, Y. Gasteuil, M. Bourgoïn, R. Volk, A. Pumir, and J.F. Pinton, *Tracking the dynamics of translation and absolute orientation of a sphere in a turbulent flow*, Rev. Sci. Instrum. 82 (2011), p. 033906.
- [6] R. Zimmermann, L. Fiabane, Y. Gasteuil, R. Volk, and J. Pinton, *Measuring Lagrangian accelerations using an instrumented particle*, preprint(2012). Available at arXiv, arXiv:1206.1617.
- [7] S. Klein, M. Gibert, A. Bérut, and E. Bodenschatz, *Simultaneous 3D measurement of the translation and rotation of finite size particles and the flow field in a fully developed turbulent water flow*, Meas. Sci. Technol. 24 (2013), p. 024006.
- [8] D. Vincenzi, *Orientation of non-spherical particles in an axisymmetric random flow*, J. Fluid Mech. 719 (2013), pp. 465–487.
- [9] S. Parsa, E. Calzavarini, F. Toschi, and G. Voth, *Rotation rate of rods in turbulent fluid flow*, Phys. Rev. Lett. 109 (2012), p. 134501.
- [10] T.J. Pedley and J.O. Kessler, *Hydrodynamic phenomena in suspensions of swimming microorganisms*, Annu. Rev. Fluid Mech. 24 (1992), pp. 313–358.
- [11] M.R. Maxey and J.J. Riley, *Equation of motion for a small rigid sphere in a nonuniform flow*, Phys. Fluids 26 (1983), p. 883.
- [12] E. Calzavarini, R. Volk, M. Bourgoïn, E. Leveque, J. Pinton, and F. Toschi, *Acceleration statistics of finite-sized particles in turbulent flow: The role of Faxén forces*, J. Fluid Mech. 630 (2009), p. 179.
- [13] H. Homann and J. Bec, *Finite-size effects in the dynamics of neutrally buoyant particles in turbulent flow*, J. Fluid Mech. 651 (2010), p. 81.

- [14] G. Voth, A. la Porta, A. Crawford, J. Alexander, and E. Bodenschatz, *Measurement of particle accelerations in fully developed turbulence*, J. Fluid Mech. 469 (2002), pp. 121–160.
- [15] N.M. Qureshi, M. Bourgoïn, C. Baudet, A. Cartellier, and Y. Gagne, *Turbulent transport of material particles: An experimental study of finite size effects*, Phys. Rev. Lett. 99 (2007), p. 184502.
- [16] A. La Porta, G. Voth, A. Crawford, J. Alexander, and E. Bodenschatz, *Fluid particle accelerations in fully developed turbulence*, Nature 409 (2001), pp. 1017–1019.
- [17] F. Toschi, L. Biferale, M. Cencini, E. Calzavarini, A. Lanotte, and J. Bec, *Heavy particles in turbulent flows RM-2007-GRAD-2048.St0. iCFDdatabase. Dataset.*, 2011. Available at <http://dx.doi.org/10.4121/uuid:a64319d5-1735-4bf1-944b-8e9187e4b9d6>.
- [18] L. Biferale, G. Boffetta, A. Celani, A. Lanotte, and F. Toschi, *Particle trapping in three-dimensional fully developed turbulence*, Phys. Fluids 17 (2005), p. 021701.